Appendix A: MERA Tensor Networks

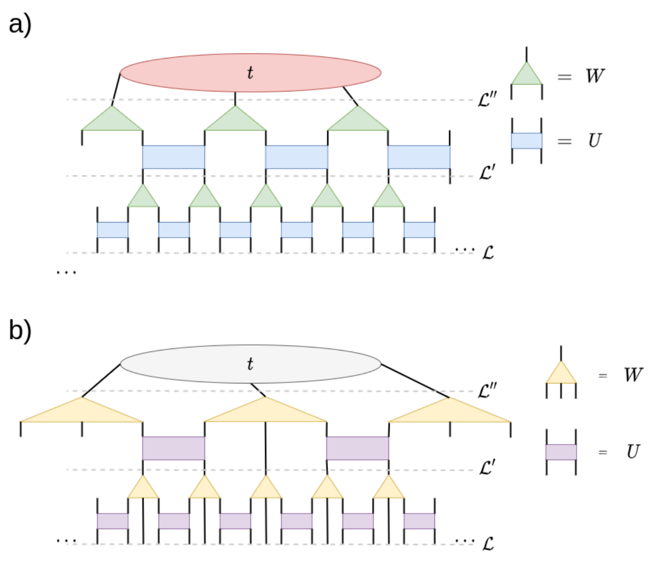

FIG. 8. Subfigures a) and b) show the binary MERA and the ternary MERA implementations [8–12]. Top tensors are shown as tensors t in the figure, whereas the isometries and unitaries are identified by key.

The *multiscale entanglement renormalization ansatz* (MERA) has attained much success as a tensor-network ansatz that implements real-space renormalization group techniques in order to facilitate the study of *scale-invariance* and *quantum criticality* in the context of quantum lattice models. Several varieties of MERA-family tensor networks are shown in the Figure 8 ; however, for the purposes of this article, we shall focus our attention on *binary* MERA and *ternary* MERA. The basic idea of these tensor networks is the same; a MERA tensor network consists of several types of tensors:

1) Top Tensors:

$$t = U\left|0\right\rangle\left|0\right\rangle, (t)_{\mu\nu} = (U)^{\alpha\beta}_{\mu\nu}|_{\alpha,\beta=0}, \quad \text{(A1)}$$

where two indices are contracted, and each top tensor corresponds to a two-body unitary operator. The top tensor is normalized to one;

2) Isometries:

$$\sum_{\mu\nu} W^{\mu\nu}_{\alpha} W^{\alpha'}_{\mu\nu} = \delta_{\alpha\alpha'}, \quad \text{(A2)}$$

if only 2 indices are contracted,

$$\sum_{\alpha} W^{\mu\nu}_{\alpha} W^{\alpha}_{\mu'\nu'} = \mathcal{P}^{\mu\nu}_{\mu'\nu'}, \quad \text{(A3)}$$

in the case of 1 index being contracted;

and 3) Disentanglers:

$$\sum_{\mu\nu}(U^*)^{\mu\nu}_{\alpha\beta}(U)^{\alpha'\beta'}_{\mu\nu} = \sum_{\mu\nu} U^{\mu\nu}_{\alpha'\beta'}(U^*)^{\alpha\beta}_{\mu\nu} = \delta_{\alpha\alpha'}\delta_{\beta\beta'}, \quad \text{(A4)}$$

where the disentanglers are simply unitarity gates[8, 9].

These tensors are organized in a hierarchical fashion with the goal of implementing a local, *real-space* renormalization group transformation; in the scale-invariant version of MERA, all of the set of $\{U, W\}$ that comprise the network are defined to be exactly the same. This renormalization group flow can be described as

$$(\mathcal{L}, \hat{H}) \rightarrow (\mathcal{L}', \hat{H}') \rightarrow (\mathcal{L}'', \hat{H}'') \rightarrow \ldots, \quad \text{(A5)}$$

where $\mathcal{L}'$ refers to the first effective lattice generated upon promoting an operator (such as the locally separable Hamiltonian $\hat{H}$ in the equation below) to a higher layer, inside of the bulk of the MERA network.

An important stipulation for realizing the RG flow in MERA comes from the restrictions on the Hamiltonian. In MERA, it is assumed that the Hamiltonian can be broken down into a sum of nearest-neighbor terms:

$$\hat{H} = \sum_{s} h(s, s+1), \quad \text{(A6)}$$

where $h(s, s+1) = h$ is a localized Hamiltonian term. Every portion of the lattice, then, can be viewed as completely characterizing $\hat{H}$.

Renormalization of a local operator or reduced-density matrix can be realized in either form of MERA via *ascending* and *descending* superoperators, respectively. In a typical non-scale-invariant MERA, the ascending and descending superoperators are responsible for sequentially promoting/demoting an operator up/down the MERA:

$$\mathcal{O} \xrightarrow{\mathcal{A}(\mathcal{O})} \mathcal{O}' \xrightarrow{\mathcal{A}(\mathcal{O}')} \mathcal{O}'' \xrightarrow{\mathcal{A}(\mathcal{O}'')} \ldots,$$

we see a similar expression for descending superoperators $\mathcal{D}$:

$$\ldots \xrightarrow{\mathcal{D}(\rho''')} \rho'' \xrightarrow{\mathcal{D}(\rho'')} \rho' \xrightarrow{\mathcal{D}(\rho')} \rho,$$

and we can conclude from the action of both of these superoperators that they are in fact dual to each other (in the Choi-Jamiolkowski representation of a quantum channel [7, 59, 60]):

$$\mathcal{D} = \mathcal{A}^*$$

or

$$tr\Big[\mathcal{O}_{s-1}\mathcal{D}(\rho_s)\Big] = tr\Big[\mathcal{A}(\mathcal{O}_{s-1})\rho_s\Big].$$

However, for the purposes of this paper, we consider the scale-invariant regime; as such, every step in the renormalization group calculus now maps from fixed RG point to fixed RG point. The form of the descending and ascending superoperators simplifies to that of the *scaling superoperators*, which are described as:

$$\mathcal{A}(\mathcal{O}) \mapsto \mathcal{S}(\phi_\alpha), \tag{A7}$$

which is given by

$$\mathcal{S}(\phi_\alpha) = \lambda_\alpha \phi_\alpha, \tag{A8}$$

where ϕ_α is a scaling field operator, and λ_α are the eigenvalues after application of the superoperator. Addtionally, we have that

$$\Delta_\alpha = -\log_s(\lambda_\alpha), \tag{A9}$$

where Δ_α are the scaling dimensions of a CFT, and s is the scale factor, determined by number of sites renormalized per layer. Additionally, the dual of the ascending superoperator $\mathcal{A}^*$, the descending superoperator $\mathcal{D}$, is described in the scale-invariant regime as $\mathcal{S}^*(\rho(\mathcal{R}_n))$. The scaling superoperators of a MERA can be diagonalized in order to estimate the scaling dimensions of a related CFT [7, 10–12].

The 2- and 3-point correlation functions in MERA can be calculated in order to find three-point structure constants, as well; this is done after first performing a variational optimization of the groundstate energy for a particular quantum critical model, such as the transverse-field Ising model [11, 12]. Afterwards, the two- and three-point functions are seen to have the general forms:

$$\langle \phi_\alpha \phi_\beta \rangle = \frac{\lambda_{\alpha\beta}}{|r_{xy}|^{\Delta_\alpha + \Delta_\beta}}, \tag{A10}$$

for the two-point function, and the three-point function as:

$$\langle \phi_\alpha \phi_\beta \phi_\gamma \rangle = \frac{\lambda_{\alpha\beta\gamma}}{|r_{xy}|^{\Omega^\gamma_{\alpha\beta}} |r_{yz}|^{\Omega^\alpha_{\beta\gamma}} |r_{zx}|^{\Omega^\beta_{\gamma\alpha}}}, \tag{A11}$$

where $\Omega^\gamma_{\alpha\beta} = \Delta_\alpha + \Delta_\beta - \Delta_\gamma$, $\{\phi_\alpha\}$ represent scaling operators from the relation $\mathcal{S}(\phi_\alpha) = \lambda_\alpha \phi_\alpha$, and $|r_{xy}| = |x - y|$. Although these general forms were obtained for two- and three-point functions in MERA after groundstate-energy minimization, these relations are completely general for all 2D CFTs [40, 41, 48, 61].

In [12] it was shown that the *central charge* of a $(1+1)$-dimensional CFT can be calculated using the Cardy formula for entanglement entropy [62, 63]:

$$\mathcal{S}(\rho(\mathcal{R}_n)) - \mathcal{S}(\rho(\mathcal{R}_m)) = \frac{c}{3}\big(\log n - \log m\big), \tag{A12}$$

where $n > m$, and $n, m \in \mathbb{Z}_+$. $\mathcal{S}(\rho(\mathcal{R}_n))$ is the n-site entanglement entropy, given by the von Neumann entropy $\mathcal{S}(\rho(\mathcal{R}_n)) = -Tr\big[\rho(\mathcal{R}_n)\log(\rho(\mathcal{R}_n))\big]$.

The actual reduced-density matrices in MERA are associated with *causal cones* $\{\mathcal{C}(\mathcal{R}_n)\}$ that depend on the size of the lattice that we are considering at an n-site boundary $\mathcal{R}_n$.

It was Swingle [19, 20] who first realized that some features of the AdS/CFT correspondence are similar to what is proposed in MERA; among these include the emergence of a discretized timeslice of AdS space. However, MERA is not generally seen as an *exact* discrete analog of AdS space; work from [21] pointed out that MERA actually may be more suitable as a discretized version of *de Sitter* space, rather than anti-de Sitter space. Additionally, Carroll et al. [22] showed that MERA is only capable of describing states at length scales larger than the AdS radius, and, that the inherent directionality of MERA's isometric and unitary tensors provide intractable bounds for reproducing any notion of the correspondence within the current version of MERA. Modifications of MERA, however, were not ruled out as potentially fulfilling some of the necessary requirements in order to accurately reproduce holographic state correspondences [25, 27, 64–69], as MERA was also provided an interpretation pertaining to *kinematic space discretizations* [24]. Recently, a lightcone interpretation of MERA was introduced as well [70–73].

Appendix B: Perfect Tensor Networks

After the proposal of [28], which stated that many features of holography can be reinterpreted in the language of quantum error correction, Harlow et al.[29] proposed a new class of tensor network that is based on the construction of a quantum error correction code in the tensor-network framework. The elementary building blocks of such a tensor network are *perfect tensors*, a special class of tensor that exhibits maximal entanglement along any bipartition. More succinctly, perfect tensors are defined as specific types of isometric tensors (which are defined naturally as a map $\mathcal{T}$ from one Hilbert space $\mathcal{H}_a$ to another $\mathcal{H}_b$ such that $\mathcal{T} : \mathcal{H}_a \mapsto \mathcal{H}_b$, and $dim(\mathcal{H}_a) \leq dim(\mathcal{H}_b)$), where

$$\mathcal{T} : |a\rangle \mapsto \sum_b |b\rangle\, \mathcal{T}_{ba}, \tag{B1}$$

where $\{|a\rangle\}, \{|b\rangle\}$ are the complete orthonormal bases for $\{\mathcal{H}_a, \mathcal{H}_b\}$, respectively, and

$$\sum_b T^\dagger_{a'b} T_{ab} = \delta_{aa'}, \tag{B2}$$

and

$$\sum_b T_{ab} T^\dagger_{a'b} = \mathcal{P}, \tag{B3}$$

and $\mathcal{P}$ is a projective operator. A perfect tensor, then, is defined as a tensor with $2n$ indices (where n is the number of qubits), and, for a bipartition of indices into sets:

$$\mathbb{A}| \leq |\mathbb{A}^c|, \tag{B4}$$

the magnitudes of each set must sum up to the total z:

$$|\mathbb{A}| + |\mathbb{A}^c| = z, \tag{B5}$$

and $\mathcal{T}$ must still be proportional to an isometric tensor, i.e.

$$\sum_b \mathcal{T}^\dagger_{a'b} \mathcal{T}_{ab} = C\delta_{aa'}, \tag{B6}$$

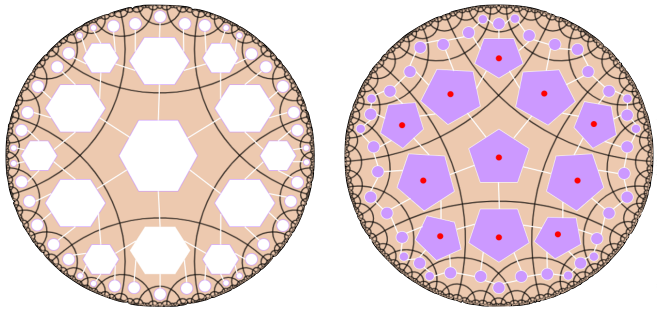

FIG. 9. Two examples of perfect tensor networks: the hexagonal state, as originally described in [29], which describes a *pure holographic state*, and the pentagonal code (also referred to as the *HyPeC* in [23, 34–36]), which contains a bulk logical index for encoding a $[[5,1,3]]$ *holographic quantum error correction code*. The HyPeC itself spurred the development of several other related *holographic tensor network codes* [74–77]. It should be noted here that the Schläfli number convention used in the perfect tensor literature follows the scheme $\{q,p\}$, whereas for hyMERA, the convention follows the form $\{p,q\}$. As such, the hexagonal state shown on the left is embedded on a $\{4,6\}$ manifold tessellation; the HyPeC is embedded on a $\{4,5\}$ manifold tessellation.

where C is a constant, and

$$\sum_b \mathcal{T}_{ab}\mathcal{T}^\dagger_{a'b} = C\mathcal{P}. \tag{B7}$$

However, not all $2n$-index states possess a perfect tensor state [53–55].

The fact that these tensor networks are comprised of perfect tensors gives the bulk portion of the tensor network a high degree of symmetry; this idea is illustrated with the concept of *bulk tensor pushing*. More simply, an operator $\mathcal{O}$ acting on an input leg of an isometric tensor can be represented by an equal-norm operator $\mathcal{O}'$ on the output leg. We see this property by the following:

$$\mathcal{T}\mathcal{O} = \mathcal{T}\mathcal{O}\mathcal{T}^\dagger\mathcal{T} = (\mathcal{T}\mathcal{O}\mathcal{T}^\dagger)\mathcal{T} = \mathcal{O}'\mathcal{T}. \tag{B8}$$

One can "push" operators through a network of perfect tensors by exploiting this characteristic. The extra symmetry of the perfect tensors in the bulk provides us with the isotropic symmetry that we seek in an actual timeslice of AdS space. This quality provides a unique advantage over MERA in terms of describing the bulk characteristics of holography. Additionally, the enhanced symmetry in the bulk allows one to define a stabilizer formalism for the purpose of encoding quantum information in the form of a quantum error correction code[29].

It has been shown that when perfect tensor networks are assigned to a bulk tessellation, associated with a strongly-disordered boundary in the form of a *conformal quasicrystal* [26], perfect tensor states can *on average* observe certain characteristics reminiscent of CFT-groundstates [23, 34, 35]. It was shown in several works that perfect tensor states can be related to Majorana dimer states [34, 35], while still retaining properties of exact quantum error correction. Indeed, such Majorana dimer-based models have been associated with critical Hamiltonians in the lattice limit [23, 35]. However, entanglement relationships in these models are typically sparse; an averaging procedure is required in order to observe CFT-like behavior. This work advances the results found in [29, 33], where n-site correlation functions previously were shown to result in either zero or a phase, without any averaging treatment. Finally, a holographic analog to the *Bacon-Shor* quantum error correction code was proposed in [78].